FLIM (Fluorescence Lifetime Imaging Microscopy) of Avocado Leaves during Slow Fluorescence Transient (the P to S Decline and the S to M Rise)

Yichun Chen[a], Shizue Matsubara[b,*], Rosanna Caliandro[b], Govindjee[c], Robert M Clegg[a,d,e]

[a]Bioengineering Department, University of Illinois at Urbana-Champaign (UIUC), Urbana, IL 61801, USA;
[b]IBG-2: Pflanzenwissenschaften, Forschungszentrum Jülich, 52425 Jülich, Germany;
[c]Department of Plant Biology, [d] Center for Biophysics and Computational Biology, UIUC , Urbana, IL 61801, USA ;
[e]Department of Physics, UIUC, Urbana, IL 61801, USA;
*Corresponding author. E-mail: ycchen.christine@gmail.com

Abstract: Fluorescence lifetime imaging measurements were made on intact avocado leaves (*Persea americana* Mill.) during the slow part of chlorophyll (Chl) *a* fluorescence transient, the P to S and the S to M phase. Contributions of lutein-epoxide and violaxanthin cycles operating in parallel on the ΔpH-dependent (transthylakoid H^+ concentration gradient) thermal energy dissipation (qE) and slowly reversible ΔpH-independent fluorescence quenching (qI) were studied. A polar plot analysis of the lifetime data revealed three major chlorophyll *a* fluorescence lifetime pools for photosystem II. The longest lifetime pool (centered at 2 ns) was observed when linear electron transport and the resulting ΔpH build-up were inhibited in leaves. The other two lifetime pools (1.5 and 0.5 ns) were observed during ΔpH build-up under illumination. Interconversion between these two lifetime pools took place during the slow part of the chlorophyll *a* fluorescence transient. Formation of the 0.5 ns pool upon illumination was correlated with dark-retention of antheraxanthin and photo-converted lutein in leaves. In the absence of ΔpH, neither the intensity nor the lifetimes of fluorescence were affected by the presence of antheraxanthin and photo-converted lutein. We conclude that both antheraxanthin and photo-converted lutein are able to enhance ΔpH-dependent qE processes associated with the 0.5 ns lifetime pool.

Keywords: Chlorophyll *a* fluorescence transient; Fluorescence lifetime imaging microscopy; Lutein epoxide cycle; Non-photochemical quenching; Violaxanthin cycle

Introduction

There are several different non-photochemical quenching (NPQ) pathways in Photosystem II (PSII) complex (Müller, 2001). They operate in tandem to regulate the efficiency of light energy absorption, and play a role in photoprotection of chloroplasts. One of the NPQ pathways is ΔpH-dependent (transthylakoid H^+ concentration gradient) thermal energy dissipation (qE), which involves the violaxanthin (V) cycle during light-driven acidification in thylakoid lumen (Demmig-Adams and Adams III, 1996; Müller *et al*., 2001). Violaxanthin is de-epoxidized to antheraxanthin (A) and zeaxanthin (Z) by the enzyme V de-epoxidase at low lumen pH, while the reverse reactions are catalyzed by Z epoxidase on the stromal side of the thylakoid and become detectable when V de-epoxidase is inactive at high lumen pH. Some higher plants have an additional xanthophyll cycle: lutein epoxide (Lx) cycle (García-Plazaola *et al*., 2007) which involves Lx and lutein (L). Lx is de-epoxidized to lutein in a similar way as the conversion from V to A and Z. However, the epoxidation from L to Lx is at a much slower rate than the V cycle. Pogson *et al*. (1998), Pogson and Rissler (2000) and Li *et al*. (2009) have suggested that L is related also to thermal energy dissipation in *Arabidopsis thaliana*, a plant without the Lx cycle to modulate L levels via xanthophyll cycling; however, the physiological functions of the Lx cycle operation and the

consequences of the slow post-illumination Lx restoration (*i.e.* prolonged retention of photo-converted L) are still under discussion (García-Plazaola *et al*., 2003; Matsubara *et al*., 2008; Förster *et al*., 2009).

In order to study the NPQ effects of the V cycle and the Lx cycle operating in parallel, we measured the fluorescence lifetime of chlorophyll (Chl) *a* during the slow part of fluorescence transient, the P (peak) to S (semi-steady state) decline and the S to M (maximum) rise (Govindjee, 1995; Papageorgiou *et al*., 2007) in real time. As the two xanthophyll cycles have different epoxidation rates, a time-course of fluorescence lifetime measurement protocol was designed. Fluorescence lifetime can reveal the state of Chl *a* undergoing dynamic quenching. Together with the fluorescence intensity data, the fractional contribution of Chl *a* at different de-epoxidation states (DPS) in the two xanthophyll cycles, and the dynamic interconversion between those states were analyzed on "polar plots" (Clayton, 2004; Redford and Clegg, 2005; Chen and Clegg, 2009). The species fraction of the observed lifetime pools was also compared with the DPS of the two xanthophyll cycles in the samples. Details of our results and their interpretations are published in Matsubara *et al*. (2011). We present here some highlights of this research.

Materials and Methods

The fluorescence lifetime measurements of avocado leaves were made by full-field frequency-domain fluorescence lifetime imaging microscopy (FLIM) (Schneider and Clegg, 1997). The frequency-domain fluorescence lifetime parameters, M and φ, were measured at every pixel. These parameters are related to a single lifetime as follows:

$$M = 1 / \sqrt{1 + (\omega\tau)^2} \quad (1)$$

$$\varphi = \tan^{-1}(\omega\tau) \quad (2)$$

where, ω is the modulation frequency of the instrument, and τ is the fluorescence lifetime of the fluorophore. FLIM images were obtained from the adaxial surface of the leaf. The excitation light (488 nm, ~50 μmol photons m^{-2} s^{-1} at the leaf surface) was obtained from a laser; PSII fluorescence emission was collected between 670 nm to 725 nm (Chen and Clegg, 2009). The fluorescence lifetime data were presented and analyzed on "polar plots" (Clayton, 2004; Redford and Clegg, 2005; Chen and Clegg, 2009). The x- and y-axes of the polar plot are defined as:

$$x = M\cos(\varphi) \quad (3)$$

$$y = M\sin(\varphi) \quad (4)$$

The advantage of a polar plot is that it provides immediate visualization and characterization of multiple lifetime data without *a priori* assuming a model.

In order to understand the mechanism of changes in the observed fluorescence lifetimes and intensities, a two-lifetime model (as in Holub *et al*., 2007) was simulated to compare with our data. Lifetime parameters used in the simulation were obtained from the polar plot analysis of our data. In the two-lifetime model, the fluorescence intensity change is due to the interconversion of the same fluorophore between two lifetime states. This simulation is able to distinguish between changes in concentration of fluorophores (related to changes in absorption cross section caused by the so-called 'state changes', chloroplast movement or chlorophyll bleaching) and changes in rate constants of de-excitation pathways (*e.g.*, excitation energy transfer, heat loss).

The protocol of the time-course of FLIM experiment is shown in Fig. 1. For FLIM measurement we took three replicate leaf discs (50 mm^2) from different leaves. The leaf disc labeled '*control*-morning' was measured at 8:30 AM in a dark-adapted state, without any prior light treatment. Other leaf discs were exposed to 20 min room light (~5 μmol photons m^{-1} s^{-1}, labeled as '*control*-treatment') or halogen lamp (400 to 500 μmol photons m^{-1} s^{-1}, labeled as '*light*-treatment') followed by different dark adaptation times: 10 min, 60 min, 180 min, and 360 min. Twenty consecutive FLIM measurements were made on each dark-adapted leaf disc. After 5 min dark-adaptation of the sample, the last (21^{st}) measurement was made. Finally, leaf discs were dark-adapted for another 5 min and frozen in liquid nitrogen for HPLC pigment analysis. Each FLIM measurement took ~15 seconds; thus, 20 continuous FLIM measurements took 5 minutes.

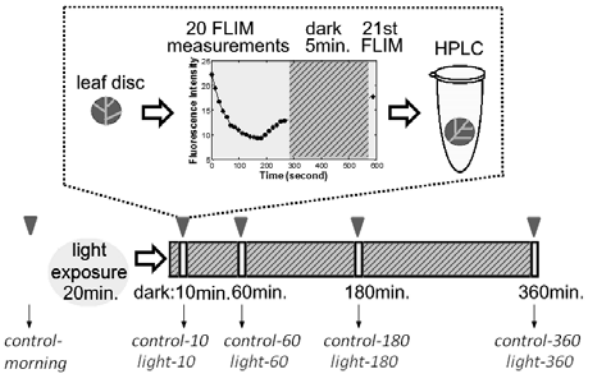

Fig. 1 The experimental protocol of the time-course of FLIM measurements used in our studies on Avocado leaves (see text, and Matsubara *et al*., 2011; with permission from Matsubara).

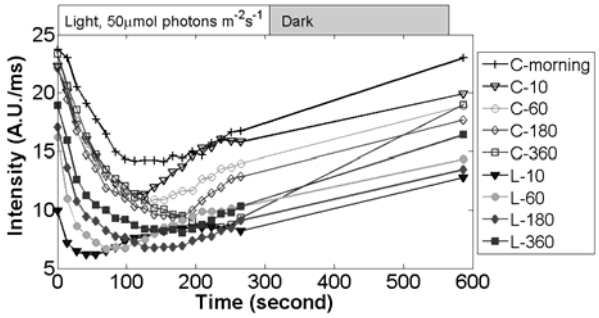

Fig. 2 Chl fluorescence intensity transients during the continuous FLIM measurements on Avocado leaves (average of three experiments). '*Control*-morning': crosses (+); other '*control*-samples': open symbols; '*light*-samples': filled (closed) symbols. Different dark adaptation time after light treatment is indicated as the number following "C" (for control) and "L" (for light). (See Matsubara *et al*., 2011; with permission from Matsubara).

Results and Discussions

Chl *a* fluorescence intensity during 20 continuous FLIM measurements under laser illumination and a subsequent 21st measurement after 5 min of dark adaptation is shown in Fig. 2. The fluorescence intensity decreases first (during the P to S phase) and then increases (during the S to the M phase) in all the samples. The '*control*-samples' start at higher intensity levels than the '*light*-samples', showing the effect of light treatment on these samples. The decreasing part of the fluorescence transient (the P to S) for the '*control*-samples' (open symbols) is essentially independent of the dark-adaptation times used (10, 60, 180, 360 min). However, the '*light*-samples' (solid symbols) vary with the same different dark adaptation times: here, the P level is lowest for the 10 min dark curve, increasing with longer dark adaptation times; even the 360 min (*light*-360) curve is still lower than the '*control*-samples'. The rising part of the fluorescence transient (the S to M phase) has slower onset time with longer dark adaptation in both the *control*- and the *light*-samples. Except for '*light*-10', the 21st measurement has the intensity level of about 80% to 90% of the 1st measurement, indicating that irreversible photoinhibition effect is not significant in our data. In '*light*-10', the 21st data has higher intensity level than that of the 1st measurement.

The fluorescence lifetime data from one of the three leaves is shown in Fig. 3. Lifetime data on the polar plot are all inside of the semicircle, indicating that there are multiple lifetimes in the sample.

As the data (Fig. 3) showed a correlation between the change in fluorescence intensity and the lifetime, we fitted them with a linear least-squares regression on the polar plot, which gives 1.5 ns and 0.5 ns values for two fluorescence lifetime pools. The two lifetimes were then used in the two-lifetime model calculation. The simulated steady-state fluorescence intensity is plotted as a function of the intensity contribution from the 0.5 ns lifetime (Fig. 3B). As the data are very close to the two-lifetime model simulation, we suggest that a reversible interconversion between the 1.5 and 0.5 ns lifetime pools is responsible for the fluorescence intensity change. The fluorescence intensity change was less affected by difference in the concentration of Chl a (*e.g.* state transitions).

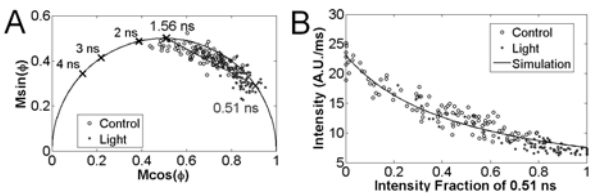

Fig. 3 Chl fluorescence lifetime data from one of the three replicates of Avocado leaves. '*Control*-samples": open circles; '*light*-samples': filled (closed) circles. (A) Polar plot representation. (B) Steady state fluorescence intensity plotted against the intensity fraction of the 0.5 ns lifetime pool. Simulation from the two-lifetime model is also shown by drawn line (Matsubara *et al*., 2011; with permission from Matsubara).

The species fraction of the short (0.5-ns) lifetime pool was also compared with the (DPS) of the two

xanthophyll cycles determined by HPLC pigment analysis.

The DPS of the V cycle is defined as ([A]+[Z])/([V]+[A]+[Z]), where [V], [A] and [Z] are the measured mmol amounts of V, A and Z per mol of Chl *a*. As Z was not detected in any of the sample, the 0.5 ns fraction was compared with [A]/([V]+[A]), as shown in Figs. 4A, 4B, and 4C. Likewise, the DPS of Lx cycle is defined as [L]/([Lx]+[L]), and the correlation with the 0.5 ns lifetime is plotted in Figs. 4D, 4E and 4F). The 0.5 ns species fraction was also compared with a combined DPS of the two cycles, ([A]+[L])/([V]+[A]+[Lx]+[L]) (shown in Figs. 4G, 4H and 4I). Linear regression lines were fitted to the data, and all of them show positive correlation. The highest R^2 values are seen between the 0.5-ns lifetime component and the DPS of the two xanthophyll cycles combined, suggesting the involvement of both the xanthophyll cycles in the interconversion between the 1.5 and 0.5 ns lifetime pools.

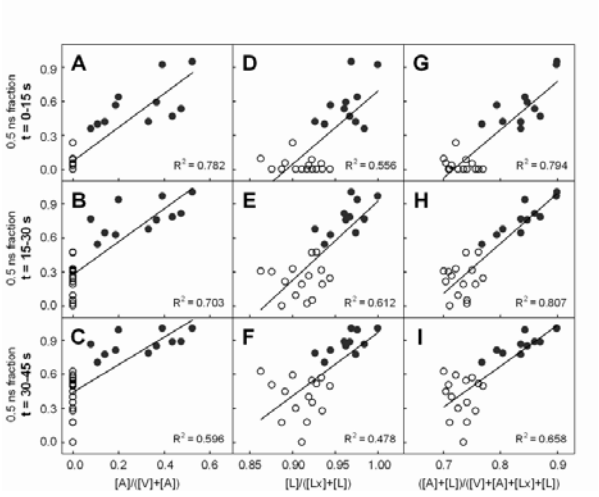

Fig. 4 Correlation between the de-epoxidation state (DPS) of the two xanthophyll cycles and the species fraction of the 0.5-ns lifetime of Avocado leaves. The 1st (t = 0 – 15 s; A, D, and G), 2nd (t = 15 – 30 s; B, E, and H), and 3rd (t = 30 – 45 s; C, F, and I) of the 21 FLIM measurements were used. '*Control*-samples': open circles; '*light*-samples': filled circles (Matsubara *et al*., 2011; with permission from Matsubara).

The linear electron flow was inhibited by 3-(3,4-dichlorophenyl)-1,1-dimethylurea (DCMU) in order to study the effects of ΔpH build-up on fluorescence lifetimes and intensity. Leaf discs were incubated in 1.2 mmol DCMU for 360 min after room light ('DCMU-*control*') or halogen lamp light ('DCMU-*light*') treatment. As shown in Fig. 5, the fluorescence intensity and the lifetime parameters remained nearly unchanged during laser illumination. The 'DCMU-*control*' and the 'DCMU-*light*' samples have very similar lifetime and intensity values. The least-squared fit of lifetime data on the polar plot gives 2.2 ns and 0.7 ns lifetime values, and the corresponding two-lifetime model simulation is shown in Fig. 5B. Interconversion between the two lifetime pools was not observed in the DCMU incubated samples.

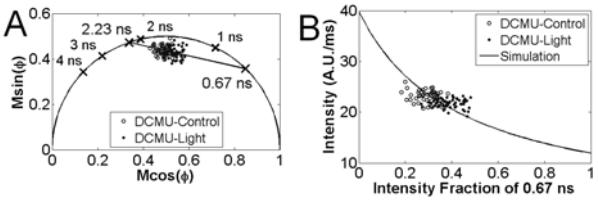

Fig. 5 When ΔpH build-up was inhibited by DCMU, the fluorescence lifetime and intensity remained constant. 'DCMU-*control*': open circles; 'DCMU-*light*': filled (closed) circles. (A) Polar plot representation. (B) Steady state fluorescence intensity plotted against the fractional contribution of the 0.7 ns lifetime pool. Simulation from the two-lifetime model is also shown here (Matsubara *et al*., 2011; with permission from Matsubara).

Conclusions

The fast data acquisition of FLIM enabled us to obtain real-time measurements of Chl *a* lifetimes during the slow part of fluorescence transient (the P to S; and S to M phase) in Avocado leaves. Formation of the 0.5 ns pool upon illumination could be correlated with the DPS of the two xanthophyll cycles due to dark-retention of antheraxanthin and photo-converted lutein in leaves. Data suggest that the presence of ΔpH is required for the quenching of fluorescence by antheraxanthin and photo-converted lutein. We show here the importance of both the V and Lx cycles in thermal energy dissipation processes in Avocado leaves.

References

Chen YC, Clegg RM (2009) Fluorescence Lifetime-Resolved Imaging. Photosynth. Res. 102: 143-155

Clayton AHA, Hanley QS, Verveer PJ (2004) Graphical Representation and Multicomponent Analysis of Single-Frequency Fluorescence Lifetime Imaging Microscopy Data. J. Microsc. 213: 1-5

Demmig-Adams B, Adams III WW (1996) The Role of Xanthophyll Cycle Carotenoids in the Protection

of Photosynthesis. Trends Plant. Sci. 1: 21-26

Förster B, Osmond CB, Pogson BJ (2009) De Novo Synthesis and Degradation of Lx and V Cycle Pigments during Shade and Sun Acclimation in Avocado Leaves. Plant Physiol. 149: 1179-1195

García-Plazaola JI, Hernández A, Olano JM, Becerril JM (2003) The Operation of the Lutein Epoxide Cycle Correlates with Energy Dissipation. Funct. Plant Biol. 30: 319-324

García-Plazaola JI, Matsubara S, Osmond CB (2007) The Lutein Epoxide Cycle in Higher Plants: Its Relationships to Other Xanthophyll Cycles and Possible Functions. Funct. Plant Biol. 34: 759-773

Govindjee (1995) Sixty-Three Years since Kautsky: Chlorophyll a Fluorescence. Aust. J. Plant Physiol. 22: 131-160

Holub O, Seufferheld MJ, Gohlke C, Govindjee, Heiss GJ, Clegg RM (2007) Fluorescenc Lifetime Imaging Microscopy of Chlamydomonas Reinhardtii: Non-Photochemical Quenching Mutants and the Effect of Photosynthetic Inhibitors on the Slow Chlorophyll Fluorescence Transients. J. Microsc. 226: 90-120

Li Z, Ahn TK, Avenson TJ, Ballottari M, Cruz JA, Kramer DM, Bassi R, Fleming GR, Keasling JD, Niyogi KK (2009) Lutein Accumulation in the Absence of Zeaxanthin Restores Nonphotochemical Quenching in the Arabidopsis Thaliana npq1 mutant. Plant Cell 21: 1798-1812

Matsubara S, Krause GH, Seltmann M, Virgo A, Kursar TM, Jahns P, Winter K (2008) Lutein Epoxide Cycle, Light Harvesting and Photoprotection in Species of the Tropical Tree Genus Inga. Plant Cell Environ. 31: 548-561

Matsubara S, Chen YC, Caliandro R, Govindjee, Clegg RM (2011) Photosystem II Fluorescence Lifetime Imaging in Avocado Leaves: Contributions of the Lutein-Epoxide and Violaxanthin Cycles to Fluorescence Quenching. doi:10.1016/j.jphotobiol. 2011.01.003

Müller P, Li XP, Niyogi KK (2001) Non-Photochemical Quenching: A Response to Excess Light Energy. Plant Physiol. 125: 1558-1566

Papageorgiou GC, Tsimilli-Michael M, Stamatakis K (2007) The Fast and Slow Kinetics of Chlorophyll a Fluorescence Induction in Plants, Algae and Cyanobacteria: a Viewpoint. Photosynth. Res. 94: 275-290

Pogson BJ, Niyogi KK, Björkman O, DellaPenna D (1998) Altered Xanthophyll Compositions Adversely Affect Chlorophyll Accumulation and Nonphotochemical Quenching in Arabidopsis Mutants. Proc. Natl. Acad. Sci. USA 95: 13324-13329

Pogson BJ, Rissler HM (2000) Genetic Manipulation of Carotenoids Biosynthesis and Photoprotection. Phil. Trans. R. Soc. Lond. B. 355: 1395-1403

Redford GI, Clegg RM (2005) Polar Plot Representation for Frequency-Domain Analysis of Fluorescence lifetimes. J. Fluoresc. 15: 805-815

Schneider PC, Clegg RM (1997) Rapid Acquisition, Analysis, and Display of Fluorescence Lifetime-Resolved Images for Real-Time Applications. Rev. Sci. Instrum. 68: 4107-4119